JOURNAL OF MAGNETIC RESONANCE, Series B 102, 103–106 (1993)

The Origin and Removal of Artifacts in 3D HCACO Spectra of Proteins Uniformly Enriched with ^{13}C

STEPHAN GRZESIEK AND AD BAX

Laboratory of Chemical Physics, National Institutes of Diabetes and Digestive and Kidney Diseases, National Institutes of Health, Bethesda, Maryland 20892

Received December 22, 1992

The three-dimensional HCACO experiment correlates the chemical shifts of the intraresidue H^α, C^α, and carbonyl (C') resonances, providing useful information during the sequential assignment procedure of isotopically enriched proteins (*1, 2*). To remove the antiphase doublet character from the C^α lineshape in this type of 3D spectrum, a constant-time version of the HCACO experiment has been proposed (*3*). Although close inspection of these so-called CT-HCACO spectra shows the presence of a large number of artifacts, for most smaller proteins these do not interfere with spectral interpretation. The observed artifacts are of opposite sign to the resonances of interest and they have much larger resonance linewidths in the C' dimension of the 3D spectrum. However, their integrated intensities are comparable to the integrated intensities of the true correlations. As was recently noted for the protein interferon-γ (*4*), for larger proteins the artifacts can interfere with spectral analysis because the fraction of residues with a high degree of internal mobility can give rise to HCACO correlations that are two orders of magnitude more intense than those for residues in the rigid core of the protein. The artifacts associated with these intense resonances therefore can obscure the presence of correlations of interest. Below we describe the origin of these artifacts and describe a simple solution to remove them.

The pulse scheme of the CT-HCACO experiment, which is functionally identical to the one described before (*3*), is shown in Fig. 1A. Although its mechanism previously has been discussed in detail (*3*), we briefly reiterate some of its essential elements in order to identify the coherence-transfer pathway leading to the artifacts. The spin operators for the H^α, C^α, C', C^β, and H^β nuclei are denoted H^α, C^α, C', C^β, and H^β, respectively. Constant multiplicative factors and terms describing relaxation have been omitted in the following description.

At time point *a* in Fig. 1A, the magnetization of interest is described by an operator product of the form $C_y^\alpha H_z^\alpha$. During the subsequent constant-time evolution period, of total duration $2T$, the C^α chemical shift evolves for a time t_1 whereas the C^α–C' and C^α–C^β J couplings are active for the full period $2T$:

$$C_y^\alpha H_z^\alpha \xrightarrow{2T,\ t_1} -C_x^\alpha H_z^\alpha C_z' \sin(2\pi J_{C_\alpha C'} T) \times \cos(2\pi J_{C_\alpha C_\beta} T)\cos(\Omega_{C_\alpha} t_1) - C_y^\alpha H_z^\alpha C_z' C_z^\beta \times \sin(2\pi J_{C_\alpha C'} T)\sin(2\pi J_{C_\alpha C_\beta} T)\cos(\Omega_{C_\alpha} t_1). \quad [1]$$

Previously (*3*), the second term on the right-hand side of expression [1] was ignored because it does not result in the resonances of interest. However, as discussed below, this term is not eliminated by the phase cycling used in the original HCACO experiment, and the relative size of the first and second term is comparable because $2\pi J_{C_\alpha C_\beta} T \approx 45°$.

If the trigonometric factors are omitted, the first term is converted at time *b* into the desired C' antiphase transverse magnetization:

$$-C_x^\alpha H_z^\alpha C_z' \xrightarrow{90°_y(C^\alpha),\ 90°_x(C')} -C_z^\alpha H_z^\alpha C_y'. \quad [2a]$$

If we assume that the C^β resonances also experience the 90° pulse applied to the nearby resonating C^α spins, the second term is transformed according to

$$-C_y^\alpha H_z^\alpha C_z' C_z^\beta \xrightarrow{90°_y(C^\alpha,\ C^\beta),\ 90°_x(C')} C_y^\alpha H_z^\alpha C_y' C_x^\beta. \quad [2b]$$

During the following t_2 evolution period, for both terms [2a] and [2b], the C' chemical shift is active, as are the C^β–C^γ, C^β–H^β, and C^α–H^α J couplings for the product on the right-hand side in expression [2b], resulting in

$$-C_z^\alpha H_z^\alpha C_y' \xrightarrow{t_2} -C_z^\alpha H_z^\alpha C_y' \cos(\Omega_{C'} t_2) \quad [3a]$$

$$C_y^\alpha H_z^\alpha C_y' C_x^\beta \xrightarrow{t_2} C_y^\alpha H_z^\alpha C_y' C_x^\beta \cos(\Omega_{C'} t_2) \times \cos^m(\pi J_{C_\beta C_\gamma} t_2)\cos^n(\pi J_{C_\beta H_\beta} t_2)\cos(\pi J_{C_\alpha H_\alpha} t_2), \quad [3b]$$

where the exponent, m, refers to the number of C^γ carbons (0, 1, or 2), and n is the number of protons attached to C^β

1064-1866/93 $5.00

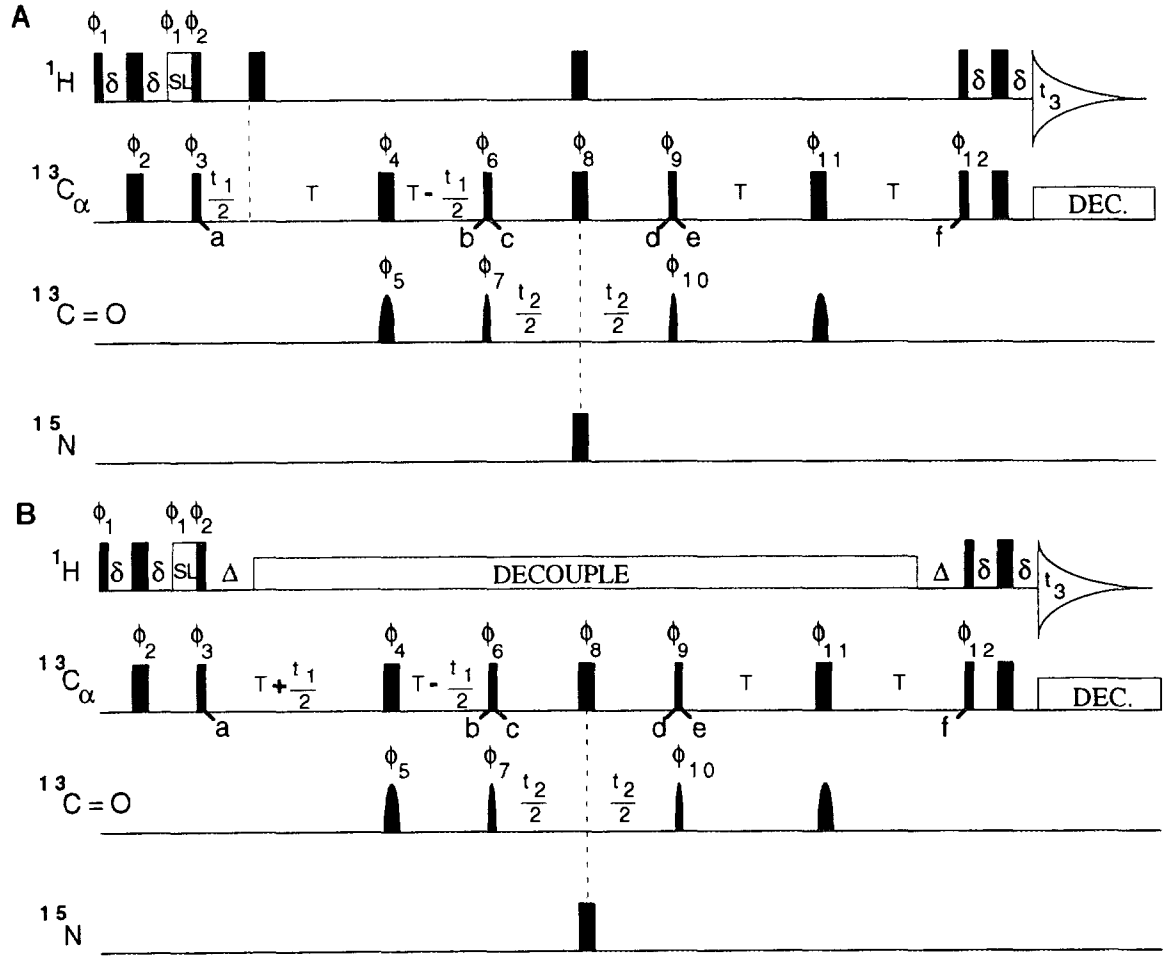

FIG. 1. Pulse schemes of the CT-HCACO experiment. Narrow and wide pulses correspond to 90° and 180° flip angles, respectively. Pulses for which the phase is not indicated are applied along the x axis. The carrier is set to the HDO frequency for the proton pulses, to 56 ppm for the $^{13}C^{\alpha}$ pulses, to 177 ppm for the carbonyl pulses, and to 116.5 ppm for the ^{15}N pulses. The power of the 90° and 180° $^{13}C^{\alpha}$ pulses is adjusted such that they do not excite the ^{13}CO nuclei (i.e., 4.7 and 10.5 kHz RF field for 150.9 MHz ^{13}C frequency, respectively). Carbonyl pulses have a shaped amplitude profile, corresponding to the center lobe of a sin x/x function and a duration of 245 μs for both the 90° and the 180° pulses. Carbon decoupling during acquisition is achieved using WALTZ-16 modulation with a 3.4 kHz RF field. The proton spin-lock pulse, SL, is applied for a duration of 1.8 ms and serves to suppress the intense HDO resonance. Delay durations are δ = 1.5 ms, Δ = 3.3 ms, and T = 3.5 ms. In sequence B, signals from glycine residues are absent for Δ = 3.3 ms. Phase cycling for scheme A is as follows: $\phi_1 = y$; $\phi_2 = x, -x$; $\phi_3 = x$; $\phi_4 = 8(x'), 8(y'), 8(-x'), 8(-y')$; $\phi_5 = 8(x), 8(-x)$; $\phi_6 = 4(y), 4(-y)$; $\phi_7 = x, x, -x, -x$; $\phi_8 = 4(x), 4(-x)$; $\phi_9 = x$; $\phi_{10} = x, -x$; $\phi_{11} = x'$; $\phi_{12} = y$; Receiver = $2(x), 4(-x), 2(x), 2(-x), 4(x), 2(-x)$. For scheme (B), the phase cycling is as above, except for $\phi_6 = 4(x), 4(-x)$ and $\phi_9 = y$. For a pure cosinusoidal t_1 modulation, the phase ϕ_4 needs to be adjusted relative to the phases of the 90° $^{13}C^{\alpha}$ pulses in order to compensate for Bloch–Siegert-induced phase errors (*9*) caused by the carbonyl 180° pulses and for phase changes caused by the change in RF power level between the 90° and 180° $^{13}C^{\alpha}$ pulses. For optimal sensitivity, the phase ϕ_{11} requires the same adjustment. In practice, this amounted to a rotation of 4° on our AMX-600 spectrometer. Quadrature in the t_1 and t_2 domains is obtained by changing the phases ϕ_3 and ϕ_7, respectively, in the usual States–TPPI manner (*14*).

(1, 2, or 3). At time point d, in the previously described version of the CT-HCACO experiment, the 90° C^{α} pulse, following the t_2 evolution period, was applied along the y axis, giving rise to

$$-C_z^{\alpha}H_z^{\alpha}C_y' \xrightarrow{90^{\circ}_x(C'),\,90^{\circ}_y(C^{\alpha})} -C_x^{\alpha}H_z^{\alpha}C_z' \quad [4a]$$

and

$$C_y^{\alpha}H_z^{\alpha}C_y'C_x^{\beta} \xrightarrow{90^{\circ}_x(C'),\,90^{\circ}_y(C^{\alpha},\,C^{\beta})} -C_y^{\alpha}H_z^{\alpha}C_z'C_z^{\beta}. \quad [4b]$$

After rephasing of the ^{13}C–^{13}C J coupling during the subsequent delay $2T$, between time points e and f, one obtains

$$-C_x^{\alpha}H_z^{\alpha}C_z' \xrightarrow{2T} -C_y^{\alpha}H_z^{\alpha}\cos(2\pi J_{C\alpha C\beta}T)\sin(2\pi J_{C\alpha C'}T) \quad [5a]$$

$$-C_y^{\alpha}H_z^{\alpha}C_z'C_z^{\beta} \xrightarrow{2T} C_y^{\alpha}H_z^{\alpha}\sin(2\pi J_{C\alpha C\beta}T)\sin(2\pi J_{C\alpha C'}T). \quad [5b]$$

The $C_y^{\alpha}H_z^{\alpha}$ terms on the right-hand side of expressions [5a] and [5b] are converted into observable H^{α} magnetization

by the subsequent reverse INEPT sequence. Therefore, both pathways that exist during the t_2 evolution period give rise to observable H^{α} magnetization. Also, as can be seen from expressions [5a] and [5b], for $t_2 = 0$ the pathway that involved three-spin coherence (expressions [2b]–[5b]) gives rise to magnetization that is of opposite sign to the desired pathway.

As is evident from expression [3b], the undesired pathway is modulated not only by the C′ chemical shift, but also by the C^{α}–H^{α}, C^{β}–H^{β}, and C^{β}–C^{γ} J couplings. Therefore, the undesired pathway results in a multiplet structure in the F_2 dimension of the 3D spectrum. For threonine residues, for example, a triplet is expected, caused by the $^1J_{C\alpha H\alpha}$ splitting which is superimposed on the splitting caused by $^1J_{C\beta H\beta}$. Superimposed on this triplet is still the smaller (~37 Hz) $^1J_{C\beta C\gamma}$ splitting. As pointed out above, the entire multiplet is antiphase with respect to the desired H^{α}–C^{α}–C′ cross peak. An example of the superposition of the desired HCACO singlet and the artifactual multiplet is shown in Fig. 2A.

As is clear from the above discussion, the structure of the spurious multiplet depends on the type of amino acid. For threonine, with only one H^{β} proton, the structure has the appearance of a triplet with a superimposed small $^1J_{CC}$ splitting. For serine residues, with two H^{β} protons and no $^1J_{C\beta C\gamma}$ coupling, the multiplet is a quartet (Fig. 2C). Although one could consider the spurious multiplet as informative, as its structure contains information regarding the type of amino acid, this information can be obtained more effectively from a range of other experiments (*5–9*). As discussed below, the negative peaks can be removed simply by changing by 90° the phase of the last two 90° $^{13}C_{\alpha}$ pulses in the scheme in Fig. 1A.

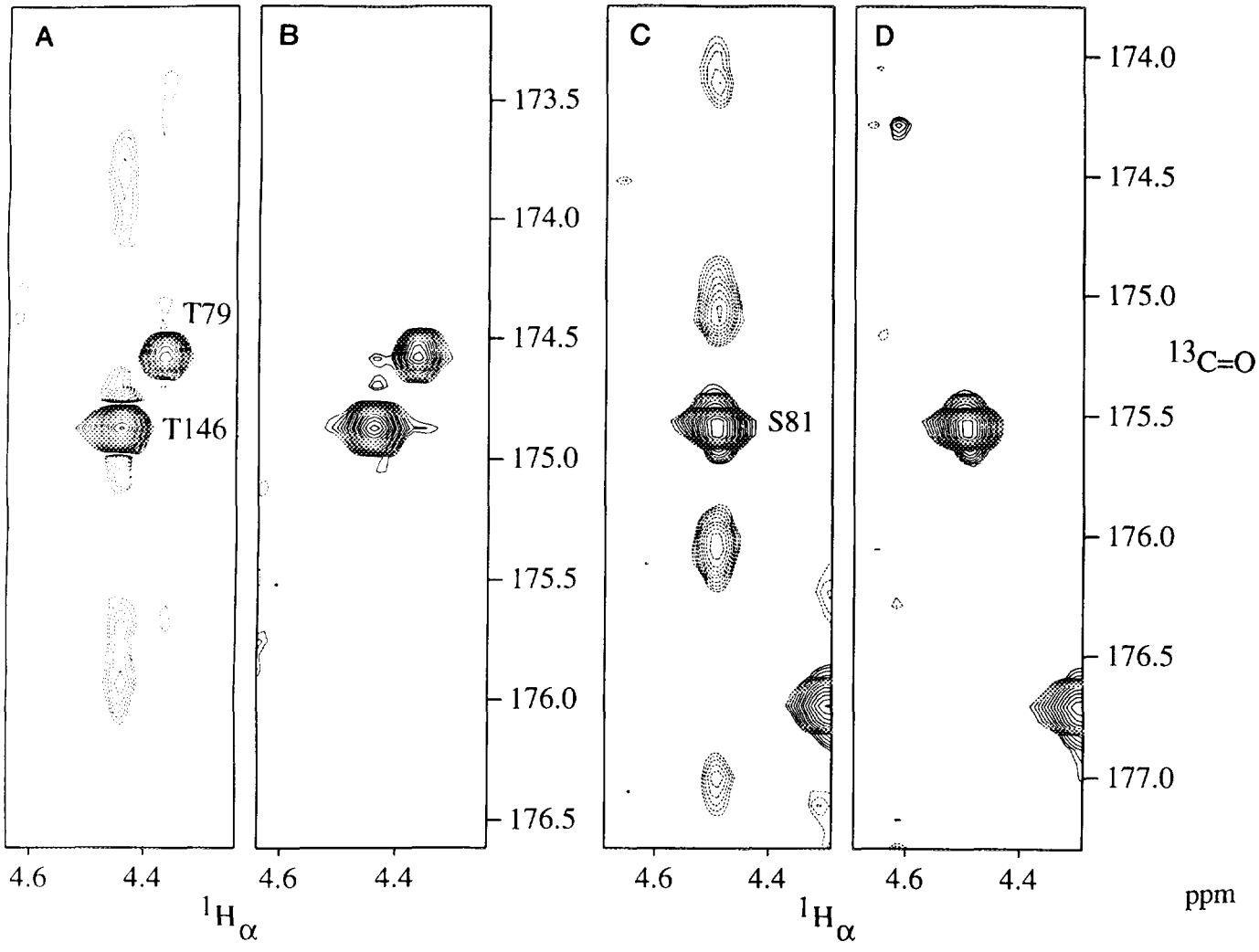

FIG. 2. Small sections of $^1H^{\alpha}$–^{13}CO planes of a HCACO spectrum recorded with the pulse scheme in Fig. 1A for the protein calmodulin, taken at a $^{13}C^{\alpha}$ frequency of 62.6 ppm (A, B) and at 59.5 ppm (C, D). Spectra A and C have been recorded with the old phase setting of $\phi_9 = y$ and $\phi_{12} = x$ (see text), whereas spectra B and D have been recorded with $\phi_9 = x$ and $\phi_{12} = y$. Broken contours correspond to negative intensity, associated with the artifactual multiplets discussed in the text.

If the phase $\phi_9 = x$, expression [4] becomes

$$-C_z^\alpha H_z^\alpha C_y' \xrightarrow{90_x^\circ(C'),\ 90_x^\circ(C^\alpha)} C_y^\alpha H_z^\alpha C_z' \quad [6a]$$

$$C_y^\alpha H_z^\alpha C_y' C_x^\beta \xrightarrow{90_x^\circ(C'),\ 90_x^\circ(C\alpha,\ C^\beta)} C_z^\alpha H_z^\alpha C_z' C_x^\beta. \quad [6b]$$

Apart from a change in phase of the C^α transverse magnetization, which is compensated for by the concomitant phase change of ϕ_{12}, the desired pathway [6a] is not affected and gives rise to a spectrum with the same intensity cross peaks as the pulse scheme with the original phases. As can be seen from [6b], the pathway that gave rise to the spurious multiplet is suppressed by changing the phase ϕ_9 to x; the 90_x° (C^α, C^β) pulse now causes a state of $zzzx$ order which cannot be transformed into observable magnetization by the final reverse INEPT scheme, applied at time f.

The effectiveness of suppressing the spurious magnetization-transfer pathway in the CT-HCACO experiment is demonstrated for a sample containing 1.5 mM calmodulin, uniformly enriched with ^{13}C and ^{15}N, dissolved in D_2O, p^{2}H 6.3, 37°C. Experiments were carried out on a Bruker AMX-600 spectrometer. The size of the acquired data matrix was $15^*(t_1, C^\alpha) \times 62^*(t_2, C') \times 512^*(t_3, H^\alpha)$, where n^* denotes n complex data points. Acquisition times were 6.6, 54.3, and 85 ms in the t_1, t_2, and t_3 dimensions, respectively. After digital filtering, zero filling, and Fourier transformation in the t_2 and t_3 dimensions, the length of the t_1 time domain was doubled by mirror image linear prediction (*10*). The final size of the absorptive part of the 3D matrix was 64 × 128 × 1024 points. The total duration of each 3D experiment was 18.5 hours.

The removal of the negative artifacts from the HCACO spectrum by changing the phases of the last two 90° $^{13}C^\alpha$ pulses is illustrated in Fig. 2. Figures 2A–2D show small regions of H^α/C' planes taken at the $H^\alpha/C^\alpha/C'$ frequencies of Thr-146 (Figs. 2A and 2B) and Ser-81 (Figs. 2C and 2D). The spectra in Figs. 2A and 2C are recorded with the original phases ϕ_9 and ϕ_{12} and those in Figs. 2B and 2D with the new values for ϕ_9 and ϕ_{12}. As mentioned above, the original phases yield the spurious multiplet which is antiphase with respect to the desired HCACO correlation. For threonine (Fig. 2A), the central components of the spurious multiplet overlap with the resonance of interest and therefore also lower the signal-to-noise ratio of the desired HCACO correlation. As shown in Fig. 2B, the change in phase of ϕ_9 and ϕ_{12} effectively removes the artifacts. A similar improvement is seen for the correlation of Ser-81. The spurious quartet present in Fig. 2C, due to the coupling of the C^α–C^β two-spin coherence to two H^β and one H^α spin, is absent in Fig. 2D.

The solution proposed here for removing the spurious resonances is surprisingly simple and effective. There are, however, a number of different ways to remove them, including the use of pulsed field gradients. As mentioned below, the pulse scheme in Fig. 1A also does not offer the highest possible resolution in the C' dimension and has been chosen primarily to illustrate the nature of some prominent artifacts that can occur in a number of heteronuclear experiments. In the pulse scheme in Fig. 1A, the linewidth in the $^{13}C'(F_2)$ dimension of the spectrum is determined by the relaxation of $C_z^\alpha H_z^\alpha C_y'$. Relaxation of this term is influenced by ^1H–^1H spin flips involving H^α, which can significantly increase the decay rate of the antiphase C' magnetization. If the highest possible resolution in the F_2 dimension is required, it is therefore preferable to use a scheme such as the one shown in Fig. 1B, in which this antiphase term has been refocused (*11–13*). In such a pulse scheme the relative phases of ϕ_6 and ϕ_9 are even more important, as the artifactual multiplet is then split only by the $^1J_{C\beta C\gamma}$ coupling and its center is therefore located exactly at the frequency position of the desired HCACO correlation.

ACKNOWLEDGMENT

This work was supported by a grant from the AIDS Targeted Anti-Viral Program of the Office of the Director of the National Institutes of Health.

REFERENCES

1. M. Ikura, L. E. Kay, and A. Bax, *Biochemistry* **29,** 4659 (1990).
2. L. E. Kay, M. Ikura, R. Tschudin, and A. Bax, *J. Magn. Reson.* **89,** 496 (1990).
3. R. Powers, A. M. Gronenborn, G. M. Clore, and A. Bax, *J. Magn. Reson.* **94,** 209 (1991).
4. S. Grzesiek, H. Döbeli, R. Gentz, G. Garotta, A. M. Labhardt, and A. Bax, *Biochemistry* **31,** 8180 (1992).
5. B. H. Oh, W. M. Westler, P. Darba, and J. L. Markley, *Science* **240,** 908 (1988).
6. S. W. Fesik, H. L. Eaton, E. T. Olejniczak, E. R. P. Zuiderweg, L. P. McIntosh, and F. W. Dahlquist, *J. Am. Chem. Soc.* **112,** 886 (1990).
7. L. E. Kay, M. Ikura, and A. Bax, *J. Am. Chem. Soc.* **112,** 888 (1990).
8. A. Bax, G. M. Clore, P. C. Driscoll, A. M. Gronenborn, M. Ikura, and L. E. Kay, *J. Magn. Reson.* **87,** 620 (1990).
9. S. Grzesiek and A. Bax, *J. Am. Chem. Soc.* **114,** 6291 (1992).
10. G. Zhu and A. Bax, *J. Magn. Reson.* **90,** 405 (1990).
11. A. Bax, M. Ikura, L. E. Kay, D. A. Torchia, and R. Tschudin, *J. Magn. Reson.* **86,** 304 (1990).
12. J. W. Peng, V. Thanabal, and G. Wagner, *J. Magn. Reson.* **95,** 241 (1991).
13. S. Grzesiek and A. Bax, *J. Magn. Reson.* **96,** 432 (1992).
14. D. Marion, M. Ikura, R. Tschudin, and A. Bax, *J. Magn. Reson.* **85,** 393 (1989).